(Received 24 October 2024, Accepted 5 December 2024, Scheduled 27 December 2024)

Performance Analysis of Complementary Split Ring Resonator with Improved Four Element Antenna for X Band Wireless Applications

Janani Sasikumar* and Koushick V.

Department of ECE, Vel Tech Rangarajan Dr.Sagunthala R&D Institute of Science and Technology, Chennai, India

ABSTRACT: A very compact MIMO antenna for broad-band applications which covers the complete spectrum of X-band applications is represented here. The proposed element in the represented antenna covers a total volume of around 320 mm^3. The isolation among radiating elements is improved by placing individual elements orthogonally thereby improving isolation better than 20 dB. This enhanced isolation helps to provide substantial MIMO parameters including ECC, TARC, channel capacity loss, and multiplexing efficiency. The devised antenna is compact ($0.066\lambda \times 0.066\lambda \times 0.0024\lambda\,mm^3$) printed over an FR4 substrate which is widely available concerning 6.2 GHz to 11.2 GHz wireless applications. Fabrication of the above-mentioned proposed antenna is done, and all the desired calculations are made desirably. Furthermore, the practically measured results conclude that the antenna-measured patterns well correspond to the simulated results.

1. INTRODUCTION

In wireless high data rates, the UWB system's reduced power requirements have drawn a lot of attention. The frequency spectrum of 3.1–10.6 GHz is used for ultra-wideband (UWB), thus regulated by the Federal Communication Commission [1]. The output result is said to be affected by the limited channel capacity of the UWB system. In the wireless communication sector, transmission power and bandwidth are crucial subjects because they allow for better performance for more users while utilizing the limited available frequency [2]. Some have tried to expand the operable scope by operating at higher frequencies or dynamically distributing the operable spectrum, a practice known as spectrum collaboration, to achieve greater performance [3]. Full-duplex radio and multiple-input multiple-output (MIMO) techniques are two examples of these technologies. Due to its ability to significantly increase multiplexing efficiency without requiring more frequency spectrum channel capacity, MIMO systems are more widely used. MIMO approaches offer an answer to the problems of mutual coupling, physical limitations of the antenna, and channel capacity. The transmission range and channel capacity are increased by the deployment of numerous antennas [4]. MIMO technologies promise to boost channel capacity without providing more transmission power or frequency spectrum. Numerous issues could compromise system performance, particularly in small devices, as a result of numerous restrictions placed on MIMO antenna design because of spatial limitations and mutual coupling — the electromagnetic interaction between MIMO parts [5].

With positioning the antennas near one another the fields produced by one antenna tend to alter the current distribution of various radiating elements. Consequently, the presence of additional components determines the impedance matching and radiation pattern allocated to each MIMO element [6]. The MIMO system's performance is undermined by the electromagnetism between the antenna elements. It is a single multiport antenna design problem since all of the radiating components have to be contained in a single aperture [7]. Compact devices are not compatible with the conventional array design approach, which holds that a single antenna element can be created and then combined into an array topology. To lessen the reciprocal coupling impact of the antennas, several researchers employ a multi-port decoupling or matching network [8]. It is evident that MIMO radiating elements need to have multiple ports and that isolated, well-paired ports are preferable distinct applications, however, would have distinct design requirements. For example, base stations may not have space constraints related to antenna size. This will be a more pleasant implementation but is not feasible for a much more constrained application. Researchers have employed several novel strategies, including parasitic elements, neutralization lines, deformed ground structure, and electromagnetic band-gap (EBG) arrangements, to reduce electromagnetic interactions and provide enough separation between radiating elements [9, 10].

Very basic knowledge cannot be used by the designers of MIMO antennas unless they are aware of how the modes affect the antenna's performance parameters. Recent literature has looked into the application of modal analysis for antenna design and analysis. The potential and applicability of characteristic mode theory have been greatly enhanced by all of

* Corresponding author: Janani Sasikumar (jananisasikumar2701@gmail.com).

TABLE 1. Dimensional parameters.

Parameters	L	K	L1	K1	L2	K2	L3	K3
Values (mm)	20	20	5.625	2.358	1.98	3.475	1.05	3.558

these studies. The typical mode's linearity and orthogonality have some applications in the design of MIMO systems. Each mode can be excited as a MIMO channel, resulting in very minimal mutual coupling across other ports. Different modes can be sorted individually [11]. Recent literature on modal analysis for MIMO antennas has shown some amazing designs. A number of them employed the chassis mode, which necessitates numerous cuts and attempts to arrive at an ideal design [5]. The metamaterial transmission lines have found recent use in many applications, including mutual coupling reduction for numerous antenna designs, filters, absorbers, couplers, and absorbers MIMO antennas, etc., in the terahertz, millimeter-wave, and microwave bands because they have fascinating electrical characteristics [12].

2. PROPOSED ANTENNA DESIGN AND ANALYSIS

In this work, we employ a complementary split ring resonator (CSRR) for mutual coupling reduction in the form of a slotted stub and a circular loop resonator. We also examine MIMO antenna design from a modal perspective, i.e., by applying characteristic mode theory to obtain a physical understanding of the antenna operating principle without taking into account any specific feeding [13]. Below -20 dB, the isolation level is enhanced, exhibiting a notch pattern between 6.2 and 11.2 GHz. The substrate on which the antenna is built is widely available and in use. In an Advanced Development System (ADS), time-domain and multilayer solver analyses are used to develop the MIMO system. A thorough topology and design analysis are provided. To verify the findings of the simulation, a model is developed. When the measured and simulated findings are compared, it is found that there is a respectable level of agreement [14, 34–39].

The following is listed as the Research's Primary contributions:

- A single band MIMO antenna of size $20 \times 20 \times 0.8\,\text{mm}^3$ is fabricated, suitably used for X-band wireless and IoT applications.
- The UWB frequency ranges from 6.2 to 11.2 GHz, which is said to have a area size about $12 \times 6.9\,\text{mm}^2$.
- The devised antenna substantially offers isolation better than 20 dB within a small volume size which enhances the overall performance of the MIMO antenna.
- The devised antenna design is kept very simple as the decoupling mechanism is not involved.
- By placing the devised antenna around the corners of the substrate, the polarization diversity is said to be achieved to the desired level.

3. LAYOUT AND EXAMINATION OF 4 PORT MIMO ANTENNA

Figure 1(a) shows the proposed 4-port CSRR loaded wideband truncated coplanar waveguide (CPW) MIMO antenna for single-band applications. The commonly used FR4 substrate, measuring 20×20, is suitable to hold the four-port truncated antenna that is being suggested [15]. Since the suggested antenna uses a CPW construction, the ground plane is printed on a $20 \times 20\,\text{mm}^2$ sized FR4 substrate. The suggested antenna is made up of a $6.7 \times 12\,\text{mm}^2$ truncated rectangular radiator that is fed by a feeding element that measures $1.05 \times 3.5841\,\text{mm}^2$. To create more resonance, a rectangle-shaped CSRR slit is etched in the middle of the truncated radiator [16]. Figure 1(a) shows the structure and size details of the 4-port antenna, and Figure 1(b) shows the constructional details of Antenna 1 with CSRR structure's dimensional specifics.

For attaining high isolation and pattern diversity, the represented CSRR loaded antennas are said to be placed over the four ends of the provided substrate. The CSRR structure is composed of a 1 mm-wide rectangular strip with $L6 \times W5\,\text{mm}^2$ for the outer ring and $L7 \times W6\,\text{mm}^2$ for the inner ring [17]. The distance between inner and outer rings is W7 mm. The values obtained for the various dimensions are listed in Table 1. Using the ADS software from Keysight, parametric analysis was done, and all dimensions were completed. Every value in Table 1 is expressed in millimeters [18].

Antennas 1 to 4 depict the reflection and transmission coefficient of the proposed antenna elements in the MIMO system which cover wide band frequencies ranging from 6.2 GHz to 11.2 GHz over an impedance bandwidth of 10 dB. All the antennas are said to be placed in an orthogonal manner achieving an isolation up to 12 dB. Here, decoupling mechanism is not needed further which is said to be an added advantage [19].

Antenna 1, which is part of the proposed design, is chosen as the reference antenna because its main radiating element is a circular structure. This reference antenna achieves a resonant impedance bandwidth (the frequency range where the antenna performs well) about 10 dB, spanning from 6 GHz to 7 GHz, as reported in reference [20]. To improve its performance, the feed line of the circular strip antenna is connected to an impedance matching structure, which achieves a reflection coefficient below -20 dB (indicating excellent impedance matching). In comparison, Antenna 2 operates effectively over a resonance range of 5.2 GHz to 5.7 GHz, with a reflection coefficient less than -10 dB (indicating acceptable matching).

Figure 2(b) displays the reflection coefficient (S_{11}) as a function of frequency, comparing the performances of the antennas with and without the inclusion of an SRR (Split-Ring Resonator). The reflection coefficient is shown in dB, and the dashed horizontal line at -10 dB indicates the typical thresh-

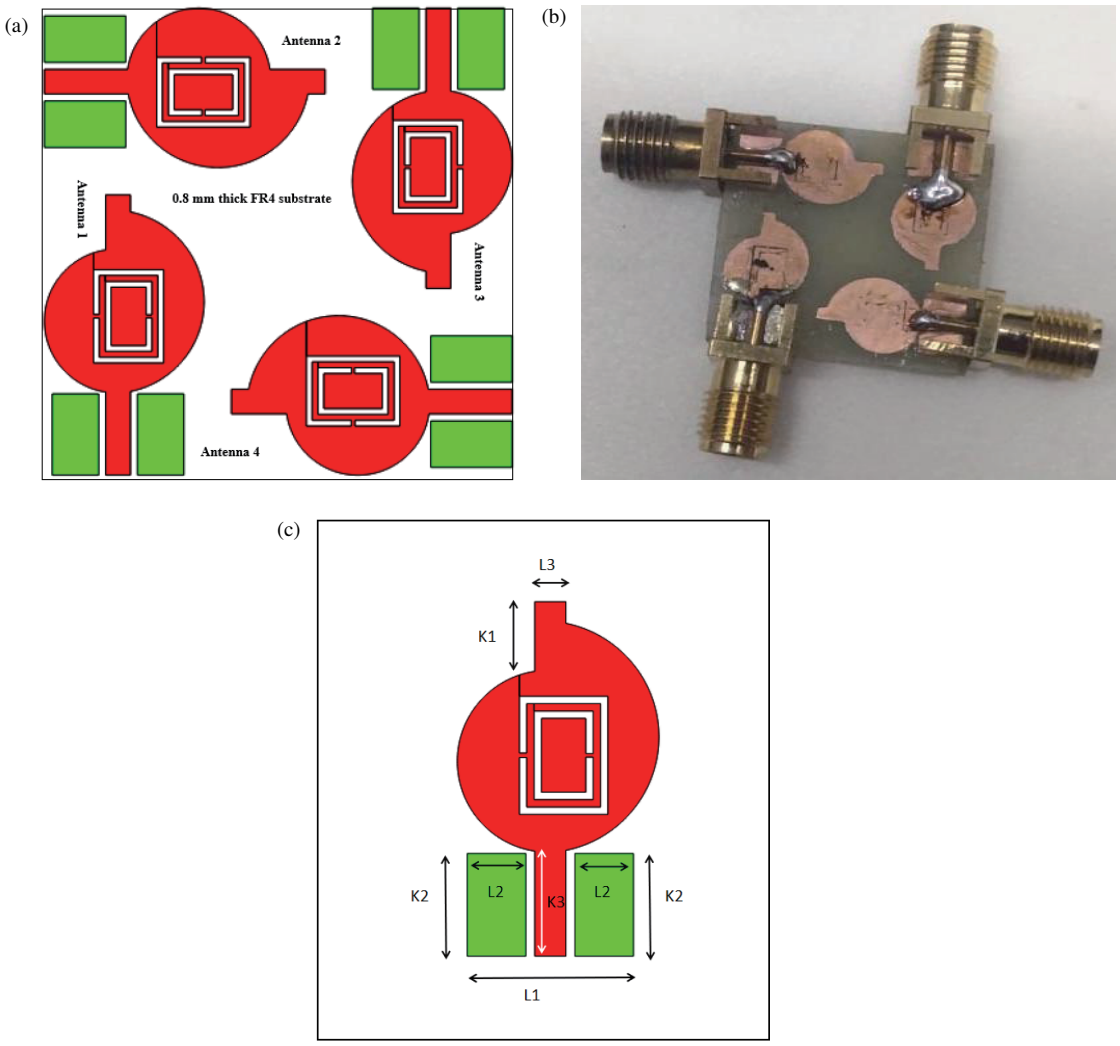

FIGURE 1. (a) Structure and size details of the 4-port antenna. (b) Fabricated prototype. (c) Constructional details of antenna 1.

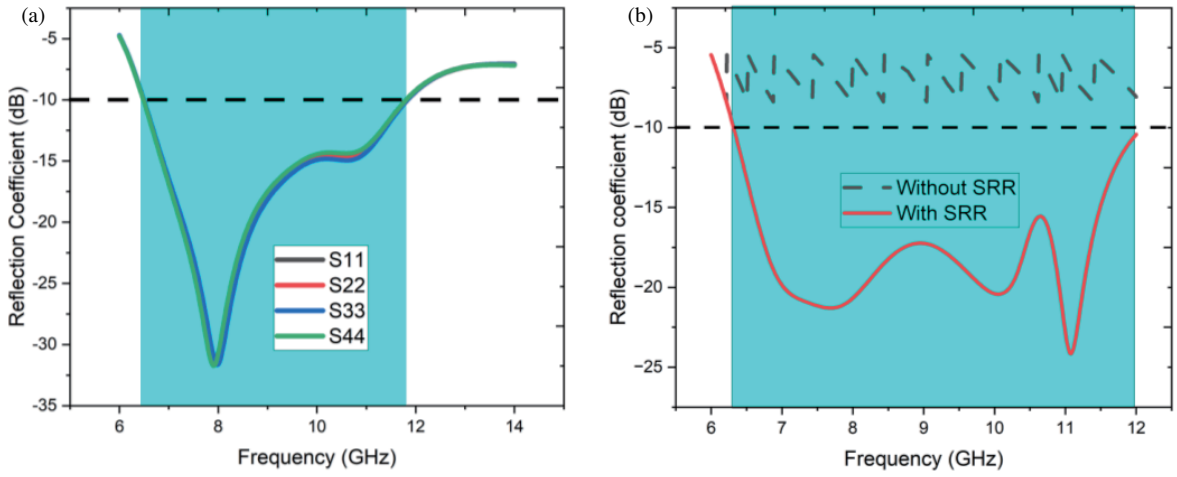

FIGURE 2. (a) Reflection coefficient of the proposed antenna. (b) Effect of SRR on reflection coefficient.

old for good impedance matching. The red curve represents the antenna with the SRR, and the black curve corresponds to the antenna without it. The results demonstrate that the antenna with SRR achieves significantly lower reflection (better impedance matching) across a wider frequency range, from 6 GHz to 12 GHz. Without the SRR, the antenna shows higher

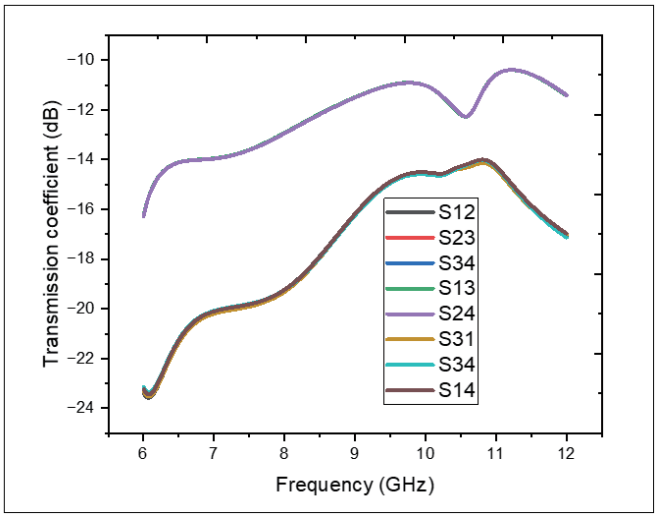

FIGURE 3. Transmission coefficient of the proposed antenna.

reflection (above -10 dB), indicating poor impedance matching and reduced performance, particularly around the resonant frequency. The inclusion of the SRR helps improve the antenna's bandwidth and overall efficiency, making it suitable for wideband applications. Figure 3 depicts the transmission coefficient of the antenna which is below -10 dB.

4. FRAMEWORK STUDY

The frequency of operation comes down by default it is shown when the height of the antenna increases [21]. Identical responses were recorded with the feed length ($L4$) which is gradually increased in increments of 0.5 mm. The antenna is said to be wideband where the response is recorded, as shown in the figure, in terms of the feed length.

The ground plane is changed from 1 to 4 mm in terms of 0.5 mm in each phase as in Figure 4(b). When $L2$ is decreased, the responses of both the higher band and lower band are fully impaired. Figure 5 presents radiation efficiency of the antenna ranging from 40 to 60% over the operating spectrum, and gain of the antenna is illustrated in Figure 6. It ranges between 7 and 7.6 dBi over the operating spectrum.

Figures 7(a) and (b) show the comparison between simulated and measured radiation patterns of Antennas 1 and 2, respectively. However, some discrepancies between the simulated and measured results can be observed, especially in the fluctuations around 7 GHz and 9 GHz, where the measured gain is slightly lower than the simulated values. These variations could be attributed to fabrication tolerances, measurement inaccuracies, or environmental factors during testing. Despite these differences, the overall trend indicates that the antenna performs well, with the simulated and measured results showing reasonable correlation, confirming the validity of the design.

To understand the polarization variations, three-dimensional pattern of the devised antenna (aligned in the X-axis) is shown. Similarly, Antenna 2 (aligned along the Y-axis) exhibits an enhanced radiation pattern along the X-axis, where the radiation intensity is observed to be significantly high. This behavior is also observed for Antennas 3 and 4, following a similar pattern as described in [24]. Hence, the polarization is achieved by positioning the antennas in a way that is distinct from one another resulting in improved isolation results [25].

5. DIMENSIONAL OUTCOME AND CONSIDERATION

The top and bottom views of the devised antenna are shown, as it is loaded with a 4 port metamaterial CSRR antenna with the applicable results.

Reflection coefficient and transmission coefficient are measured using Keysight's FirefoxNetwork Analyzer. The wide band frequency operation lavishly proves that the calculated results directly match the simulation results [26]. However, small variations or fluctuations in the measured results are found due to conducting losses caused by soldering [27].

The radiation pattern and cross polarization which is $<$ 30 dB are exhibited with the proposed antenna as it yields bidirectional radiation pattern [28]. The proposed metamaterial loaded antenna exhibits a significant gain about 2–2.5 dB. Hence, profoundly the above values validate that the proposed antenna is suitable for the desired applications mentioned [29].

6. PERFORMANCE OF MIMO ANTENNA

The performance of the MIMO antenna is improved as the isolation of the antenna is lowered. Observing the S-parameters, the performance of the devised antenna generates the required envelope correlation coefficient (ECC).

$$\rho_e = \frac{\left|\iint \bar{F}_1 \cdot \bar{F}_1^{\star} d\Omega\right|^2}{\iint \left|\bar{F}_1\right|^2 d\Omega \cdot \iint \left|\bar{F}_2\right|^2 d\Omega} \tag{1}$$

From Figure 8(a), all the ECC values within the frequency range are said to be acceptable, lower than 0.035 as shown. Overall performance of the devised antenna is validated [30]. The signal-to-noise ratio (SNR) of the devised antenna system can be improved with the diversity ratio of the MIMO antenna. To achieve the SNR level, diversity gain (DG) is a key measure to achieve it, and it is plotted in Figure 8(b).

$$DG\,(a,b) = 10\sqrt{1-ECC_{a,b}} \tag{2}$$

The channel capacity loss is an essential data transmission parameter of the MIMO antenna, determined using the equation below (3)

$$\text{Channel Loss}\,(CL) = -\log_2 \det(\varphi^R) \tag{3}$$

$$\varphi^R = \begin{bmatrix} T_{11} & \cdots & T_{14} \\ \vdots & \ddots & \vdots \\ T_{41} & \cdots & T_{44} \end{bmatrix} \tag{4}$$

where,

$$T_{ii} = 1 - \left(\left(U_{ii}^2\right) + \left(U_{ij}^2\right)\right)$$

$T_{ij} = -\left(U_{ii}^{*} U_{ij} + U_{ji}^{*} U_{jj}\right)$ for $i, j = 1, 2 \ldots 4$.

Throughout the whole spectrum, the channel capacity loss (CCL) value is said to be maintained < 0.4 bits/sec/Hz, which

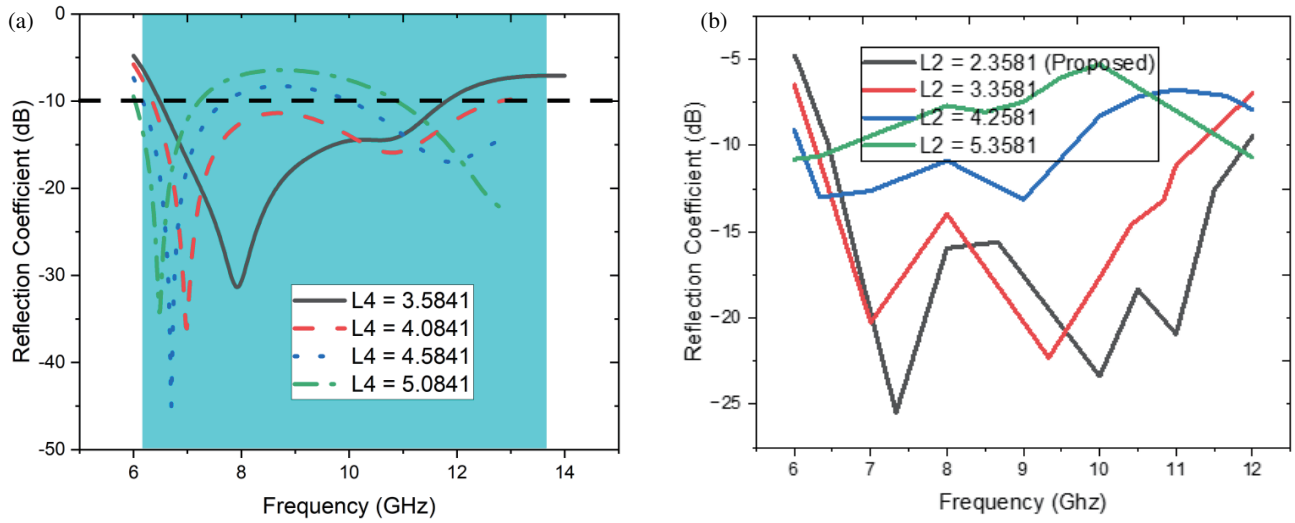

FIGURE 4. Parametric study when altering, (a) $L4$, (b) $L2$.

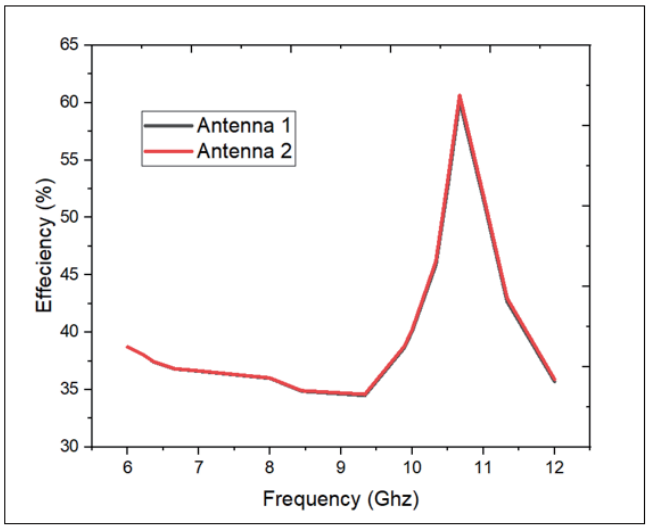

FIGURE 5. Efficiency of the proposed antenna.

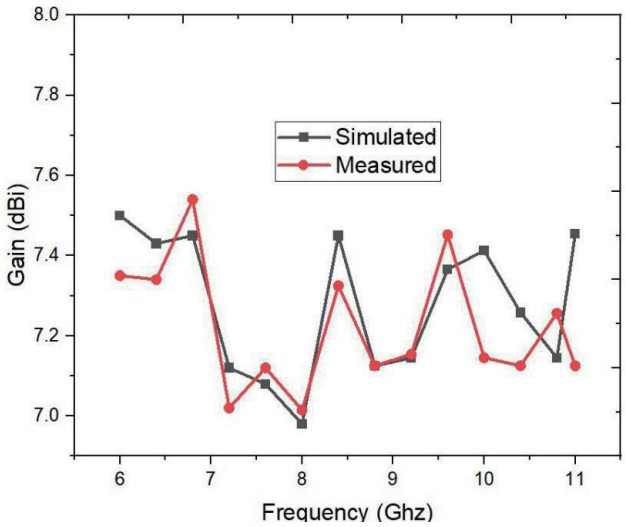

FIGURE 6. Gain of the proposed antenna.

is constant on behalf of the results along with the devised antenna capacity loss also being calculated [31]. Validating the performance of the MIMO antenna channel capacity is considered as the main factor. Considering the 20 dB SNR environment the channel capacity of individual antenna elements is calculated [32]. Single Input Single Output Antenna whose channel capacity is closer to 0.3 bps/Hz is ideal for the 4×4 MIMO antenna. Thus, the essential ECC, DG, CLL, and channel capacity are measured from the devised MIMO antenna.

A brief comparative study is done in Table 2 to prove that the devised antenna stands out from the MIMO antenna. Hence examining the performance, six features have been discussed, and comparison is made with the existing antennas. The concluded results that the overall dimensions of the proposed antenna are very much smaller than the other existing antennas [33]. The devised antenna occupies a total area about $20 \times 20 \times 0.8\,\text{mm}^2$, whose individual antenna size is about $12 \times 5.625\,\text{mm}^2$ which is smaller than all the other existing antennas. Antenna which is isolated plays a vital role in MIMO antenna as the greater the isolation length is between the antennas, the better the resulting isolation would be and vice versa.

The devised MIMO antenna achieves the good isolation of 20 dB, with the antennas strategically placed and an integrated decoupling mechanism to further enhance isolation. The devised antenna resonance is 6.2 to 11.2 GHz which is proved to be better than the existing antennas discussed in literature. The desired band of operation is found to be 0.1, and the gain is about 2.5 dB.

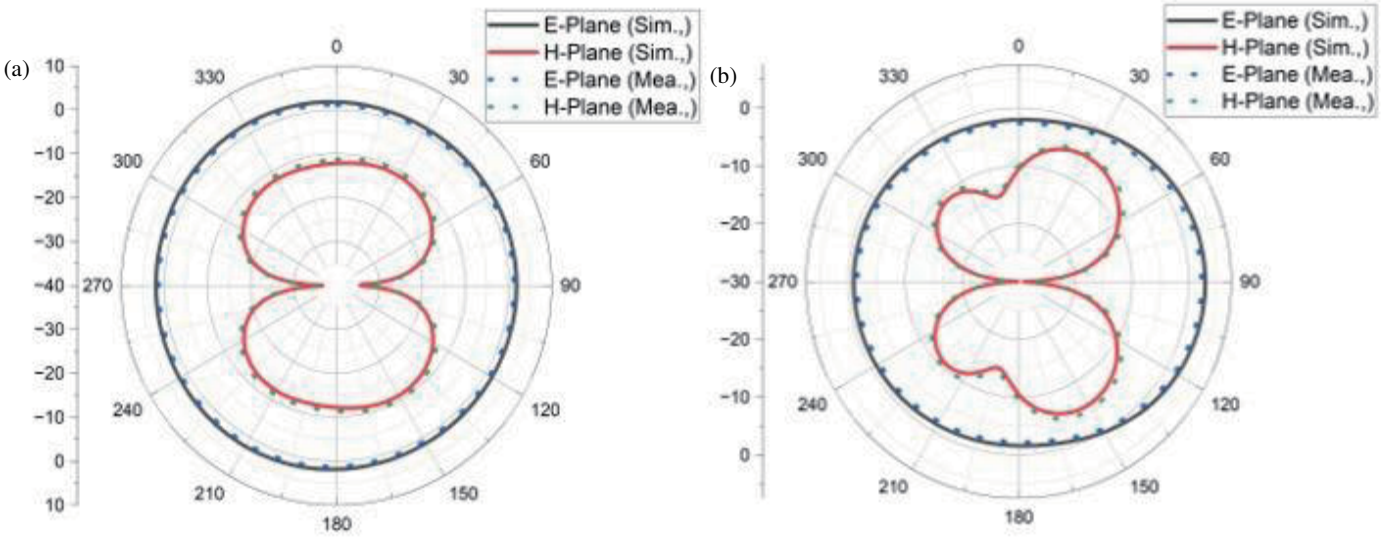

FIGURE 7. Simulated and measured far-field patterns of (a) Antenna 1. (b) Antenna 2.

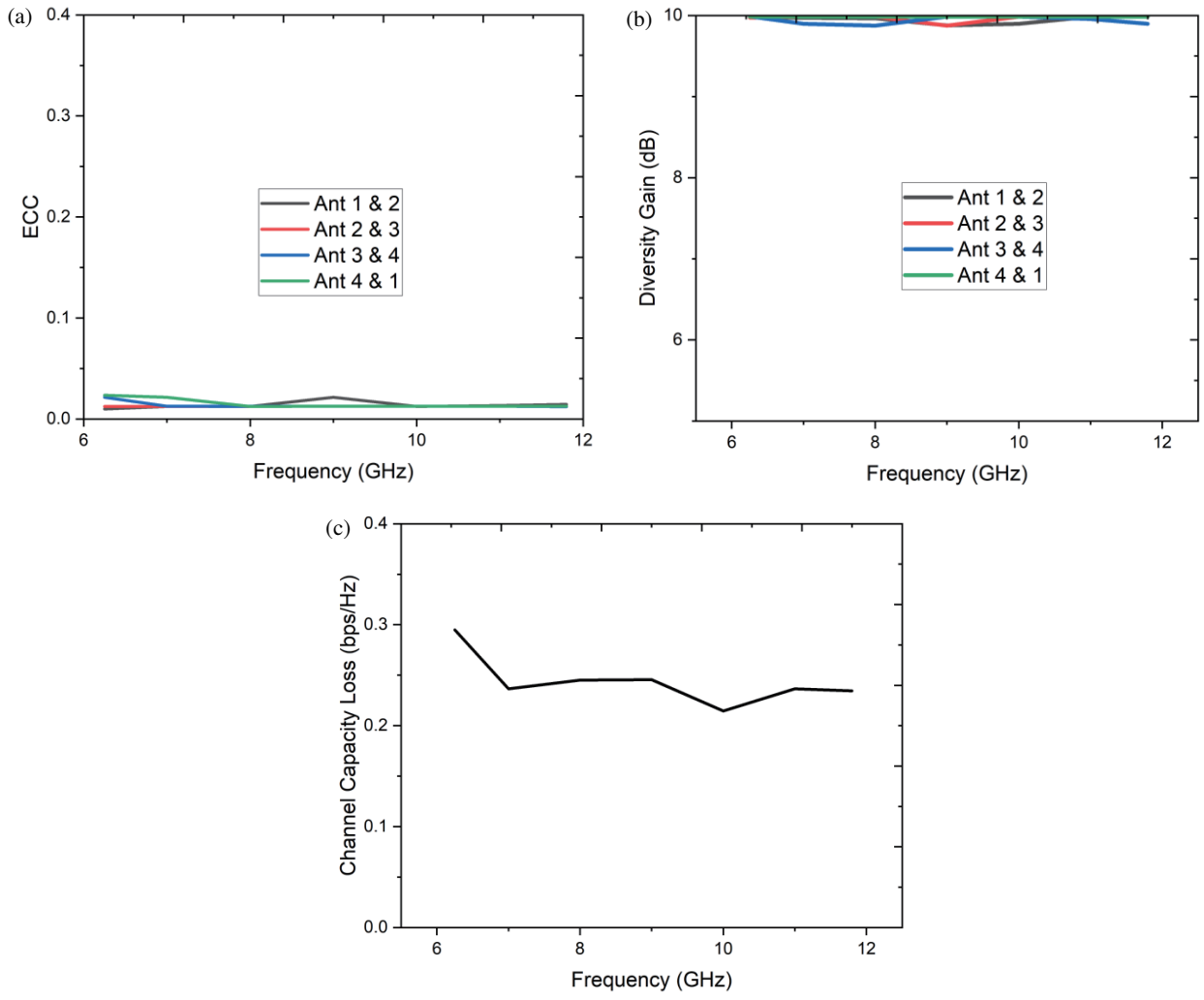

FIGURE 8. MIMO parameters. (a) ECC. (b) Diversity gain. (c) Channel capacity.

TABLE 2. Performance comparison of the proposed antenna with the literature.

S. No	MIMO antenna Size	MIMO antenna Size in terms of wavelength (λ)	Individual antenna size (mm^2)	Individual antenna size in terms of wavelength (λ)	Isolation (dB)	Operating Frequency (GHz)	ECC	Gain (dB)
[11]	60×90	$0.49\lambda \times 0.735\lambda$	17×21	$0.138\lambda \times 0.1715\lambda$	18	2.45	NA	0.55
[12]	100×50	$0.816\lambda \times 0.408\lambda$	18×14	$0.147\lambda \times 0.1143\lambda$	10	2.45	NA	NA
[13]	61×61	$0.498\lambda \times 0.498\lambda$	—	—	28	2.45	< 0.3	3.8
[14]	60×60	$0.49\lambda \times 0.498\lambda$	—	—	22	2.45	< 0.4	3.4
[15]	42×42	$0.77\lambda \times 0.77\lambda$	22×16	$0.403\lambda \times 0.293\lambda$	10	5.5	NA	5
[16]	140×120	$1.09\lambda \times 0.94\lambda$	15.5×8	$0.121\lambda \times 0.062\lambda$	15	2.35	NA	NA
[18]	40×40	$0.446\lambda \times 0.446\lambda$	27×18	$0.3015\lambda \times 0.201\lambda$	10	3.35	NA	7.9
[19]	50×50	$0.408\lambda \times 0.408\lambda$	—	—	17.5	2.45	< 0.5	2.1
[20]	100×60	$0.703\lambda \times 0.422\lambda$	15×8	$0.1055\lambda \times 0.056\lambda$	NA	2.119 & 17.55	0.04	8
[21]	60×60	$0.49\lambda \times 0.49\lambda$	22×17	$0.179\lambda \times 0.138\lambda$	17	0.875, 1.75, 1.822, 2.45	< 0.05	-2
[22]	52×52	$0.676\lambda \times 0.676\lambda$	20×20	$0.26\lambda \times 0.26\lambda$	20	3.4 & 3.9	< 0.5	6
[26]	25×25	$0.54\lambda \times 0.54\lambda$	10.485×7.5	$0.22\lambda \times 0.1625\lambda$	25	5.5 & 6.5	< 0.1	2.2–2.5
This Work	20×20	$0.73\lambda \times 0.73\lambda$	5.625×12	$0.20625\lambda \times 0.44\lambda$	20	6–11.5	< 0.1	3.5–7

7. CONCLUSION

A compact 4-port antenna loaded with a CSRR for wideband applications (6E or X-band) has been successfully designed and analyzed. One of the key advantages of the proposed antenna is its significantly reduced dimensions, measuring just $20 \times 20 \times 0.8\,mm^3$, while achieving isolation greater than 20 dB. The antenna design is thoroughly explained, with a step-by-step evolution and detailed parametric analysis. Pattern diversity is effectively achieved by positioning the antenna elements at the corners of the FR4 substrate. The antenna's performance is validated through fabrication, with measured parameters closely aligning with the simulated results. Additionally, key MIMO parameters, such as (ECC < 0.01), (CCL < 0.4), and (DG < 10 dB), are evaluated from both simulated and measured results.

REFERENCES

[1] Mishra, P., M. P. Singh, and S. Ghosh, "A compact dual band millimeter-wave CSRR loaded MIMO antenna array system for 5G applications," in *2022 IEEE Microwaves, Antennas, and Propagation Conference (MAPCON)*, 1188–1192, Bangalore, India, Dec. 2022.

[2] Suguna, N. and S. Revathi, "SRR & CSRR loading on monopole antenna for extreme wide band sub-mm wave and THz applications," in *2021 IEEE International Conference on Mobile Networks and Wireless Communications (ICMNWC)*, 1–6, Tumkur, Karnataka, India, Dec. 2021.

[3] Varma, J. S., J. R. Panda, G. Anjaneyulu, S. K. Dash, and S. Sahu, "V-shaped asymmetric slit patch antenna for wireless applications loaded with dual complementary split ring resonators," in *2023 International Conference on Artificial Intelligence and Applications (ICAIA) Alliance Technology Conference (ATCON-1)*, 1–3, Bangalore, India, Apr. 2023.

[4] Soundarya, G. and N. Gunavathi, "Customized BC-CSRR loaded patch antenna for satellite communication," in *2020 International Conference on Computer Communication and Informatics (ICCCI)*, 1–4, Coimbatore, India, Jan. 2020.

[5] Wattakeekamthorn, K., T. Wattakeekamthorn, C. Mahatthanajatuphat, P. Akkaraekthalin, and D. Torrungrueng, "Impedance matching optimization for GPS frequency band based on CSRR load technique neighboring triangular slot antenna," in *2021 18th International Conference on Electrical Engineering/Electronics, Computer, Telecommunications and Information Technology (ECTI-CON)*, 77–80, Chiang Mai, Thailand, May 2021.

[6] Nandakumar, M., K. A. Ansal, A. B. Murali, N. Cleetus, and L. Anil, "A CPW fed meandered metamaterial loaded antenna for wireless applications," in *2021 2nd International Conference on Advances in Computing, Communication, Embedded and Secure Systems (ACCESS)*, 1–5, Ernakulam, India, Sep. 2021.

[7] Parashar, R., Y. Bhomia, D. Soni, and R. K. Saraswat, "A multi-band antenna for WLAN and WiMAX wireless applications," in *2020 IEEE 9th International Conference on Communication Systems and Network Technologies (CSNT)*, 1–4, Gwalior, India, Apr. 2020.

[8] Kulkarni, J., C.-Y.-D. Sim, B. Garner, and Y. Li, "A dual-CP quad-port MIMO antenna with reduced mutual coupling for X-band application," *IEEE Antennas and Wireless Propagation Letters*, Vol. 22, No. 9, 2085–2089, May 2023.

[9] Feng, B., J. Lai, Q. Zeng, and K. L. Chung, "A dual-wideband and high gain magneto-electric dipole antenna and its 3D MIMO system with metasurface for 5G/WiMAX/WLAN/X-band applications," *IEEE Access*, Vol. 6, 33 387–33 398, Jun. 2018.

[10] Khan, I., K. Zhang, L. Ali, and Q. Wu, "A compact FSS based four-port MIMO antenna for low mutual coupling," *IEEE Antennas and Wireless Propagation Letters*, Vol. 22, No. 12, 2836–2840, Aug. 2023.

[11] Tang, Z., X. Wu, J. Zhan, S. Hu, Z. Xi, and Y. Liu, "Compact UWB-MIMO antenna with high isolation and triple band-notched characteristics," *IEEE Access*, Vol. 7, 19 856–19 865, Feb. 2019.

[12] Zheng, Q., Q. Zhao, Y. Qu, X.-x. Yang, and X. Pang, "Wideband and wide-angle RCS reduction of MIMO antennas using compensate-layered metasurface for cube satellite applications," *IEEE Transactions on Antennas and Propagation*, Vol. 72, No. 8, 6491–6499, Jul. 2024.

[13] Li, Z., C. Yin, and X. Zhu, "Compact UWB MIMO Vivaldi antenna with dual band-notched characteristics," *IEEE Access*, Vol. 7, 38 696–38 701, Mar. 2019.

[14] Rajesh, G. and R. Poonkuzhali, "Design and analysis of CPW fed ultrathin flexible MIMO antenna for UWB and X-band applications," *IEEE Access*, Vol. 12, 96 704–96 717, Jul. 2024.

[15] Chen, Z., W. Zhou, and J. Hong, "A miniaturized MIMO antenna with triple band-notched characteristics for UWB applications," *IEEE Access*, Vol. 9, 63 646–63 655, Apr. 2021.

[16] Zhang, K., Z. H. Jiang, W. L. Zhou, P. Peng, and W. Hong, "A compact, band-notched ultra-wideband fully-recessed antenna with pattern diversity for v2x communications," *IEEE Open Journal of Antennas and Propagation*, Vol. 3, 1302–1312, Nov. 2022.

[17] Jayant, S. and G. Srivastava, "Close-packed quad-element triple-band-notched UWB MIMO antenna with upgrading capability," *IEEE Transactions on Antennas and Propagation*, Vol. 71, No. 1, 353–360, Nov. 2022.

[18] Hemalatha, T. and B. Roy, "Low-profile CO-CSRR and EBG loaded tri-quarter circular patch EWB MIMO antenna with multiple notch bands," *IEEE Open Journal of Antennas and Propagation*, Vol. 5, No. 3, 634–643, Mar. 2024.

[19] Khan, A., S. Bashir, S. Ghafoor, and K. K. Qureshi, "Mutual coupling reduction using ground stub and EBG in a compact wideband MIMO-antenna," *IEEE Access*, Vol. 9, 40 972–40 979, Mar. 2021.

[20] Zhang, E., A. Michel, M. R. Pino, P. Nepa, and J. Qiu, "A dual circularly polarized patch antenna with high isolation for MIMO WLAN applications," *IEEE Access*, Vol. 8, 117 833–117 840, Jun. 2020.

[21] Jabire, A. H., H. M. Alkhoori, A. Ghaffar, Y. S. Faouri, A. Dahir, and M. I. Hussein, "Frequency and pattern reconfigurable CPW-fed MIMO antenna with multiband and wideband characteristics," *IEEE Access*, Vol. 12, 120 165–120 180, Aug. 2024.

[22] Kumar, D. R., T. Sangeetha, K. G. S. Narayan, G. V. Babu, V. Prithivirajan, and M. S. K. Manikandan, "A miniaturized CPW-fed CSRR-loaded quad-port MIMO antenna for 5.5/6.5 GHz wireless applications," *International Journal of Microwave and Wireless Technologies*, Vol. 16, No. 1, 167–176, 2024.

[23] Farooq, M. U., H. M. Saleh, M. Zahid, and Y. Amin, "Dual band scorpion-shaped antenna for 5.8 GHz ISM band and X-band applications," in *2023 7th International Multi-Topic ICT Conference (IMTIC)*, 1–4, Jamshoro, Pakistan, May 2023.

[24] Patel, A., T. Kumar, and M. S. Parihar, "A SIW cavity backed dual band filtenna for X-band and Ku-band applications with controllable radiation nulls," in *2023 IEEE Region 10 Symposium (TENSYMP)*, 1–5, Canberra, Australia, Sep. 2023.

[25] Barzegari, R., C. Ghobadi, J. Nourinia, and M. Shokri, "A dual-band dipole array antenna with fan-beam characteristics for C- and X-band applications," *IEEE Access*, Vol. 11, 67 330–67 338, Jul. 2023.

[26] Phaneendra, C. N., K. V. V. Ram, D. Naveen, L. Sreekar, and K. K. Naik, "Design a multi-band MIMO patch antenna at X, K, and Ku band for wireless applications," in *2022 Fourth International Conference on Emerging Research in Electronics, Computer Science and Technology (ICERECT)*, 1–6, Mandya, India, Dec. 2022.

[27] Bhuiyan, A. N. and M. A. Matin, "A new frequency reconfigurable antenna for S-band, C-band and X-band applications," in *2021 2nd International Conference for Emerging Technology (INCET)*, 1–4, Belagavi, India, May 2021.

[28] Tripathi, S. K. and B. B. Tiwari, "Design of a reconfigurable slot antenna for WiMAX, C-band, and X-band applications," in *2023 First International Conference on Microwave, Antenna and Communication (MAC)*, 1–4, Prayagraj, India, Mar. 2023.

[29] Venkatachari, D., S. Sahu, and N. K. Darimireddy, "Dual band symmetrical semi cylindrical DRA with patch antenna for C and X-band applications," in *2024 IEEE Wireless Antenna and Microwave Symposium (WAMS)*, 1–3, Visakhapatnam, India, Feb. 2024.

[30] Ranjan, P., S. Sur, and V. K. Pandey, "Multiple mode resonator based triple band filter for WLAN, intelligent transportation system, satellite communication and X-band applications," in *2019 9th Annual Information Technology, Electromechanical Engineering and Microelectronics Conference (IEMECON)*, 247–250, Jaipur, India, Mar. 2019.

[31] Chandra, A., S. Aswath, N. Kishore, and V. Varun, "Dual polarized CPW-fed multi-band antenna for 5G, ISM, and X-band applications," in *2024 Control Instrumentation System Conference (CISCON)*, 1–6, Manipal, India, Aug. 2024.

[32] Undrasi, A. and V. V. Khairnar, "A compact dual-band linear-to-circular polarization conversion metasurface for X-band and Ku-band applications," in *2023 IEEE Microwaves, Antennas, and Propagation Conference (MAPCON)*, 1–4, Ahmedabad, India, Dec. 2023.

[33] Anand, R., N. Sindhwani, and A. Dahiya, "Design of a high directivity slotted fractal antenna for C-band, X-band and Ku-band applications," in *2022 9th International Conference on Computing for Sustainable Global Development (INDIACom)*, 727–730, New Delhi, India, Mar. 2022.

[34] Mishra, B., R. K. Verma, N. Yashwanth, and R. K. Singh, "A review on microstrip patch antenna parameters of different geometry and bandwidth enhancement techniques," *International Journal of Microwave and Wireless Technologies*, Vol. 14, No. 5, 652–673, 2022.

[35] Nagesh, K. N., P. K. K. Varma, B. Kumar, R. K. Singh, B. Mishra, and D. K. Singh, "4-Port MIMO antenna with novel isolator conducting structure for sub-1 GHz/sub-6 GHz and RF-energy harvesting applications," *Journal of Electromagnetic Waves and Applications*, Vol. 37, No. 13, 1082–1105, 2023.

[36] Sundaravadivel, P., D. R. Kumar, Y. Padmanaban, and O. P. Kumar, "A versatile conformal circularly polarized quad-element antenna for X-band applications," *Scientific Reports*, Vol. 14, No. 1, 27721, 2024.

[37] Jhunjhunwala, V. K., P. Kumar, A. P. Parameswaran, P. R. Mane, O. P. Kumar, T. Ali, S. Pathan, S. Vincent, and P. Kumar, "A four port flexible UWB MIMO antenna with enhanced isolation for wearable applications," *Results in Engineering*, Vol. 24, 103147, 2024.

[38] Kumar, O. P., P. Kumar, T. Ali, P. Kumar, and e. al., "A quadruple notch UWB antenna with decagonal radiator and Sierpinski square fractal slots," *Journal of Sensor and Actuator Networks*, Vol. 12, No. 2, 24, 2023.

[39] Kumar, O. P., P. Kumar, T. Ali, P. Kumar, and S. Vincent, "Ultrawideband antennas: Growth and evolution," *Micromachines*, Vol. 13, No. 1, 60, 2021.